NASA TECHNICAL MEMORANDUM

NASA TM X-71450

NASA TM X-71450

ASSESSMENT OF JETS AS ACOUSTIC SHIELDS BY COMPARISON OF SINGLE- AND MULTITUBE SUPRESSOR NOZZLE DATA

by Vernon H. Gray, Orlando A. Gutierrez, and David Q. Walker
Lewis Research Center
Cleveland, Ohio

TECHNICAL PAPER proposed for presentation at Aeroacoustic Specialists Conference sponsored by the American Institute of Aeronautics and Astronautics Seattle, Washington, October 15-17, 1973

E-7690

ASSESSMENT OF JETS AS ACOUSTIC SHIELDS BY COMPARISON OF SINGLE- AND MULTITUBE SUPPRESSOR NOZZLE DATA

by

Vernon H. Gray*, Orlando A. Gutierrez**
National Aeronautics and Space Administration
Lewis Research Center
Cleveland, Ohio

and

David Q. Walker+
The Boeing Company
Seattle, Washington

ABSTRACT

Recent 1/4 scale and engine size nozzle acoustic data, for both 37-tube and single nozzles, are used to test the jet-shielding principle. At low jet velocities the multitube nozzle total sound power approaches the equivalent of 37 single tubes (no shielding), while near-sonic and above, the small equivalent number of single tubes compares well with a geometric model of lateral radiation from only about a third of the circumference of the outer jets (nearly complete shielding). At high jet velocities, the geometric shielding hypothesis is in excellent agreement with acoustic data from which the downstream coalesced jet-noise is excluded. Present results are compared with an existing correlation for single jets, and with previous publications on multijet shielding.

INTRODUCTION

Jet engine exhaust noise suppressor nozzles have undergone a variety of forms since the first tooth-type devices investigated by the British(1,2) and by the NACA(3). Among the early nozzle configurations tested were the multilobe and segmented lobe(4), the multitube(4,5), and the slot and multislot(6,7). In more recent years, an endless variety of tubes, spokes, chutes, plugs, flutes, annuli, etc. have been tested. During the effort to quiet the Boeing supersonic transport, the multitube design for suppressor nozzles was developed into a leading contender because of its large noise suppression capability and relatively low values of thrust loss.

---

* Head, Section A, Jet Acoustics Branch, Member AIAA

** Aerospace Research Engineer, Jet Acoustics Branch

+ Senior Engineer, Commercial Airplane Group

The noise suppression achieved by multi-element nozzles, particularly multitube arrays, has been thought to result from such effects as: rapid mixing; jet interactions; shock interactions; refractions; and shifts in frequency. Also, a jet-shielding effect has been postulated[5,8,9] in which the noise from central jets in a cluster is shielded in some fashion from the far field by the jets in the outer row or periphery of the cluster. This hypothesis of shielding has remained rather speculative, largely because of the manner in which data have been taken.

Customarily, multitube nozzle noise suppression values are obtained by comparing the sound from a multitube nozzle with that from a circular convergent nozzle of equivalent total area. Such comparisons lead to relationships between one large nozzle and many smaller ones. From such relations have come explanations of jet noise suppression in terms of mixing of ambient air into the cores of the smaller jets in a shorter axial distance, and hence a shorter high-velocity jet noise-generating zone. In addition, the use of smaller nozzles causes a Strouhal shift of peak noise to higher frequencies that attenuate more than low frequencies in travelling a given distance through the atmosphere.

Recent data obtained by Boeing[10] under a NASA contract allow the jet-shielding concept to be quantitatively evaluated in a different way for one type of configuration. In this systematic test program, single nozzles with the same dimensions as individual tubes in multitube nozzle arrays were tested acoustically over the same range of flow conditions as were the multitube nozzles. Nozzles with 37 tubes were tested on both a J75-engine test facility and at one-quarter-scale on a hot air flow rig. In this paper, noise from a single jet will be directly compared with the total noise from the multitube array to determine an "equivalent number of single tubes" to be used in assessing the possible shielding effects of jets. By comparing one with many nozzles of the same size in this way, the above explanation of suppression based on mixing in a shorter distance, along with Strouhal frequency shift, is no longer applicable. Furthermore, by comparing total sound power levels, the effects of refractions are eliminated from the results. The suppression mechanisms that remain as possibilities are shock interactions and various effects that can loosely be termed shielding.

The object of this paper is to demonstrate the above rationale using the new data, to present a geometric hypothesis for shielding, to compare this hypothesis with the data, and finally to use the results to draw conclusions about the shielding mechanism.

SHIELDING HYPOTHESIS

Previous Relationships

A few researchers have noted previously that multitube bundles generate less total noise than the total of all the tubes taken separately. Various expressions for the "equivalent" number of single tubes (assuming all

of the same diameter) have been attempted. Eldred, et. al.[8] offered the following empirical relation:

$$\text{"Effective" number of tubes} = (R_2/R_1) + 0.18\, N_p - 1 \qquad (1)$$

where R_2 = Radius of circle circumscribing the tube bundle

R_1 = Radius of individual tube

N_p = Number of tubes in outside row of tube bundle

Middleton and Clark[11] later suggested joining the centers of the outer tubes with straight lines and treating any noise generated by jets within the resulting polygon as "ineffective"; this approach yielded the following expression for the number of externally radiating tubes:

$$\text{Number of "complete" tubes} = (N_p/2) + 1 \qquad (2)$$

where N_p, again, is the number of outer tubes.

Motsinger and Sieckman of General Electric, in a currently unpublished analysis, observe that Eldred's equation (1) overpredicts the number of effective tubes (based considerably on Boeing SST multitube suppressor nozzle data[12], and suggest in essence dividing Eldred's prediction by the particular nozzle pressure ratio.

Present Hypothesis

The present study is based upon the 37-tube hexagonal suppressor nozzle configuration shown in Figure 1[10]. The flow and acoustic tests were performed with a model scale suppressor nozzle having tubes each nominally 1-inch in diameter (1.08-inch I.D.), and also with a geometrically similar full-scale J-75 engine suppressor nozzle with tubes each 4.3-inch in inside diameter. Tube-to-tube gaps for both configurations were approximately two-thirds of the tube diameters. Single 1-inch and 4.3-inch diameter tube nozzles were also tested for comparison with the 37-tube nozzles.

Geometric relations for the present acoustic shielding hypothesis are shown in Figure 2 for part of an outer row of jets. Jet cores and mixing zones are shown for an outer set of tubes, with cross-sections at two axial locations illustrating the spreading outer mixing zones. The basic premise is that noise generated within the jet cluster cannot radiate through the outer mixing zone of an outer jet. (The possible mechanism causing such shielding will be discussed later.) In order to achieve shielding, it is further assumed that the spreading initial mixing zones of adjacent outer jets merge together and form a "scalloped" shield (as in Section A-A)

upstream of the axial location of maximum noise generation. Likewise, the spreading outer mixing zones are assumed to persist farther downstream than does the region of maximum noise generation. However in some cases, as will be shown later, the multijets combine downstream into a large coalesced jet that becomes the dominant noise source.

Taking equal tube diameters and uniform gap spacing for the outer row of tubes, and referring to Figure 2, it is therefore hypothesized that the dominant noise reaching the far field radiates through only the dihedral angle θ of the outer jets that are arranged in a straight line, plus an additional angle at the corners. For a hexagon, the six 60° corners form the equivalent of one full 360° jet. The corners also represent the equivalent of one complete jet for any polygonal or circular array of outer tubes, because a circular array of N_p tubes can be considered a polygon of N_p sides and N_p corners. Accordingly, the general expression for the equivalent number of single tubes, representing all the noise from a multitube cluster, is

$$N = 1 + \frac{\theta}{360} N_p \tag{3}$$

(Symbols are defined in the NOMENCLATURE section.)

At the merging point of the mixing zones (Section A-A, Fig. 2), $\theta = 120°$, or 1/3 of a jet periphery, for any gap dimension or tube diameter. As the jets flow downstream, the outer mixing zones expand and θ becomes smaller, as shown in Section B-B. The angle θ is defined by two plane rays coming from one outer jet centerline and each tangent to the outer edge of the mixing zone of an adjacent coplanar jet. At $\theta = 90°$, these points of tangency coincide with the intersection points, i (Section B-B, Fig. 2) of neighboring mixing zones. Downstream of this station, θ is defined by rays through these intersection points, as the outer mixing zones continue to spread ($\theta < 90°$).

Equation (3) can be rewritten using simple trigonometry to include as variables the distance from jet exit in tube diameters, x/D, the jet spreading slope, S, and the tube-to-tube gap/diameter ratio, g/D, as follows:

For $120° \geq \theta \geq 90°$,

$$\theta = 2\left[90° - \sin^{-1}\left(\frac{1/2 + S(x/D)}{1 + g/D}\right)\right] \tag{4a}$$

$$N = 1 + \frac{N_p}{180}\left[90 - \sin^{-1}\left(\frac{1/2 + S(x/D)}{1 + g/D}\right)\right]$$

For $\theta \leq 90°$,

$$\theta = 2 \sin^{-1}\left(\frac{1 + 9/D}{1 + 2S(x/D)}\right)$$

$$N = 1 + \frac{N_P}{180}\left[\sin^{-1}\left(\frac{1 + 9/D}{1 + 2S(x/D)}\right)\right] \tag{4b}$$

Values of N calculated from this equation (4) will be compared with the data[10] in a later section.

TEST RESULTS

Single and multitube suppressor nozzle data from reference 10 can be better understood by first looking at the schematic representations in Figure 3. The noise spectra shown by the two highest curves are typical of the usual comparisons of a multitube nozzle with an equal-area circular convergent nozzle. The region between these two curves represents the amount of noise suppression obtained. The resulting multitube suppressor spectrum (solid curve) frequently displays two peaks in the distribution. The higher frequency peak (at 3) aligns with the peak of the jet spectrum (dash-dot curve) from a single element (tube) of the multitube cluster, tested separately. This peak (3) is higher in frequency than that for the equal-area nozzle (at 2), as the single element diameter is much less than the diameter of the nozzle equal in area to the total area of the individual elements. The peak which sometimes develops in the multitube spectrum at (1) is lower in frequency even than that for the equal-area jet. This peak (1) is caused by the noise from the large diameter downstream jet, which is the coalescence of all the individual jets. Thus, the multitube spectrum can be visualized as the sum of two spectra, a and b, (extensions dotted) where (a) represents the initial mixing region of the individual jets with the atmosphere, and (b) is the downstream coalesced jet region.

Sound Power Data

Sound power spectra from reference 10 are shown in Figure 4 for single- and 37-tube nozzles and for engine and quarter scales. The peak frequencies of the single tube nozzles are approximately the same as the higher frequency peaks of the 37-tube nozzles. At the higher pressure ratios the 37-tube nozzles exhibit the low frequency peaks caused by the coalesced jets. From these plots and the other applicable data, a single frequency best separating these peaks into two spectral regions for later analysis was selected as 400 Hz for the engine scale data and 1600 Hz for the quarter scale model data. These frequencies correspond to the intersection points of curves (a) and (b) of Figure 3. At low pressure ratios, evidence of turbine noise appears in the engine scale multitube data, and

also some unidentified low frequency (internal ?) noise appears in the quarter scale suppressor nozzle data.

The variations with Strouhal number of the normalized power spectral densities for representative single and multitube nozzle data are shown in Figure 5 for both nozzle scales. These distributions are based on the diameter D of the individual tube, whether in a cluster or single. The curves all peak at Strouhal numbers between 0.1 and 0.2, again illustrating common frequencies in the initial mixing region. The coalesced jet region is indicated by the high power densities at low Strouhal numbers. At the pressure ratio of 2.4, the engine and quarter scale data agree well in this region, but do not at 1.4 pressure ratio because of the turbine and possible internal noise mentioned before.

Parametric variations of total sound power (integrated over all frequencies) for the single- and 37-tube nozzles, quarter- and engine-scale, are shown in Figure 6 in terms of the ideal jet velocity (V_{id}, see NOMENCLATURE) for temperatures from ambient to 2500° F. For several constant jet temperatures, the data cover a range of pressure ratios from 1.4 to 4.0.

Inspection of the data slopes in Figure 6 in terms of powers of jet velocity indicates the following:

(a) The single nozzles show variance closely approaching the eighth power at low pressure ratios,

(b) At higher pressure ratios, the single nozzles vary to a higher power at the lower temperatures, due to shock noise,

(c) At higher temperatures and pressure ratios, the single nozzles vary to a power gradually decreasing from eight, as is customary,

(d) The quarter scale multitube nozzle at low pressure ratios varies at less than eighth power, and at high pressure ratios at more than eighth power. This could indicate some internal noise at low pressure ratios, but subsequent analysis will relate it to variations with velocity in the shielding ability of a multijet cluster,

(e) The engine scale multitube nozzle was tested along the J-75 engine operating line rather than at constant temperatures, so velocity powers are not directly obtainable from these data.

The data of Figure 6 will be used later to determine equivalent number of single tubes (N) for the multitube nozzles.

Correlation of Sound Power Level Data

The sound power level data of Figure 6 are compared with previous single jet noise data in Figure 7 by plotting the data according to the correlation method of reference 13. The single tube data for both scale sizes

are distributed along the correlation curve for single jets. The 37-tube nozzle data are represented by a higher single faired curve for the quarter-scale model (Fig. 7(a)), and a still slightly higher curve is obtained for the engine scale nozzle (Fig. 7(b)).

These curves are compared with other published multitube nozzle data in Figure 8, using the same correlation technique. Suppressor nozzle data from references 12 and 14 are presented for cases with available sound power levels. The area ratio parameter shown in Figure 8 is defined as the area of the circle circumscribing the outer-most tubes divided by the total exit area of the nozzles. Roughly, these data lie in the same band with the present data. However, the referenced multitube data do not contain companion data for single tube nozzles for direct comparison to obtain values for N. Furthermore in this regard, comparison of multitube nozzle data with a generalized single jet curve such as that shown in Figures 7 and 8 is not considered sufficiently precise, especially for very small tubes, such as in the 253-tube nozzle case. Such tubes generally have length/diameter ratios much larger than in the present case, and jets from such tubes contain relatively large amounts of boundary layer flow and more parabolic velocity profiles than the ideal (flat) velocity profile expected from nozzles. Therefore it is preferred to obtain N as follows from data for specific conditions, as in Figure 6.

Equivalent Number of Single Tubes

The 37-tube nozzle data of Figure 6, when referenced to the single tube data for the same velocity and temperature conditions, yield the equivalent number of single tubes (N) according to the relation:

$$(PWL)_{37} - (PWL)_1 = 10 \log N \tag{5}$$

or,

$$N = 10^{\Delta(PWL)_T/10}$$

These results are shown for both quarter- and engine-scale nozzles as a function of ideal jet velocity in Figure 9(a), and as a function of Mach number in Figure 9(b). In general, the curves establish a major trend: at low (subsonic) jet velocities, very little shielding or other type of suppression occurs, and the multitube nozzles radiate nearly the same total sound power as 37 separate single tube nozzles; at high subsonic and supersonic speeds, the 37-tube nozzle curves reach a minimum equivalent number of tubes, ranging from about 8.5 to 6.5 (except for the ambient temperature minimum which is 11); at jet velocities above about 2000 ft/sec, the equivalent number of tubes N gradually increases again.

The engine-scale data agree with the quarter-scale model data, although they lie slightly higher in equivalent number of tubes.

The minimum values of N are approximately equal to the prediction of equation (3) taken at the initial merging point of the outer jet mixing zones, where $\theta = 120°$, $N_p = 18$, and $N = 7$. Although equations (3) and (4) indicate N will decrease from this value, the data of Figure 9 indicate that this level is about a minimum; this aspect will be analyzed later.

Effect of Velocity Definition

The equivalent number of single tubes parameter N is very sensitive to the particular definition of jet velocity used. As mentioned in regard to the small tubes in the 253-tube nozzle (Fig. 8), jet velocity profiles are not always ideal. Even the engine scale suppressor nozzle with its 4.3-inch diameter tubes with length/diameter ratio of 7.5 was subject to inlet contraction losses and boundary layer growth in the tubes. The single 4.3-inch diameter tube nozzle had similar but smaller losses, because of a better inlet contraction section and somewhat smaller tube length/diameter ratio. This problem was investigated by calculating N from equation (5) using data similar to those of Figure 6, but plotted against averaged jet-exit velocities instead of ideal jet velocities. Average velocities were obtained from pressure traverses across the quarter-scale model tube exits, and from measured mass flows and thrusts for the engine-scale nozzle. Figure 10 shows N values for the engine scale nozzle for both the ideal and the average jet exit velocity cases. The same trends are exhibited in the two cases, but the average velocity case is displaced toward lower velocities and yields larger values of N, because the shift in velocity is greater for the 37-tube nozzle than for the single-tube nozzle. Similar effects occur with the quarter-scale data.

Use of the average velocity is thought to overcorrect the data, because the ideal velocity calculation predicts values closer to the peak of the jet velocity profile, and noise tends to correlate more with the peak than the average of the velocity profile. Hence, the actual values of N probably lie somwhere between the two cases shown.

Effect of Coalesced Jet

As discussed with Figures 3, 4, and 5, the secondary peak in the multitube nozzle sound power spectra at low frequencies identifies a large coalesced jet downstream of the initial mixing region. A probable reason for the increase in equivalent number of tubes N at high jet velocities (Fig. 9) is the noise from the coalesced jet which may become dominant. To separate out the coalesced jet noise, the sound power spectrum below 400 Hz for the engine-scale suppressor nozzle was excluded from the calculation for N, and the result is shown in Figure 11 based on ideal jet velocity. The difference from the calculation with all frequencies included is small near the minimum of the curve, but increases somewhat toward either end.

At the low velocity end the difference could well be internal or background noise instead of coalesced jet noise, but at the high velocity end, the curve excluding low frequencies tends to turn downward instead of upward.

This same comparison is shown more markedly for the quarter scale model in Figure 12, for N including all frequencies, and for N with those below 1600 Hz excluded. The 1000 and 1500° F jet temperature cases shown were selected because they exhibit the greatest effects apparently due to coalesced jet noise at high velocities. Values of N in Figure 12 are calculated for average jet-exit velocities to allow comparison with the ideal velocity data shown for the same conditions in Figure 9(a), and to show that both average and ideal velocity calculations yield low values of N numbers with the low frequencies excluded. With coalesced jet noise excluded, the resulting values of N, instead of increasing to about 14 tubes, drop to values of about 4.5 tubes at the higher velocities. This indicates that the coalesced jet noise is becoming dominant, but that the initial mixing region noise is being very effectively shielded. Such results would be consistent with Θ angles less than 120°.

EVALUATION OF SHIELDING HYPOTHESIS

It is desirable at this point to compare the geometric shielding hypothesis expressed by equation (4) with the present 37-tube nozzle data presented in terms of equivalent number of tubes N. Prediction curves calculated from equation (4) for the 37-tube nozzle values of $g/D = 2/3$ and $N_p = 18$ are shown in Figure 13 as functions of x/D for two representative jet spreading slopes, $S = 1/8$ and $1/10$ (half-cone angles of 7.2° and 5.7°, respectively).

To locate the experimental data for N on Figure 13, some estimate of the x/D location of maximum noise generation is required. Such data were not obtained in the study of reference 10, but use is made of information in reference 15, in which the x/D location of maximum single jet noise generation is given as a function of jet Mach number. Pertinent values of these Mach numbers are located along the top of Figure 13. Interpolating between these values of Mach number, data are plotted for N with the coalesced jet noise excluded. The quarter-scale model data show excellent agreement with the geometric model for all but the ambient temperatures, and the engine-scale nozzle data are in quite reasonable agreement.

For comparison with previous shielding relationships, the values for the present 37-tube nozzle when substituted in equation (1) yield a constant of 13.2 "effective" tubes, and equation (2) predicts 10 "complete" tubes. For another comparison, at $x/D = 12$ and $S = 0.125$, the angle $\Theta = 49°$; this happens to be the same angle for noise radiation from outer tubes as that calculated by an entirely different method in reference 14 for an extreme case of noise suppression with a 50-tube nozzle.

The present geometric hypothesis of shielding appears to predict a floor which is the best shielding (or suppression) that is obtainable with

non-dominating coalesced jet noise, with near-ideal jet velocity conditions (nozzle discharge coefficients ≈ 1), and spacing of tubes in the outer tube row that is a good compromise between shielding and ventilation effects. To prevent the coalesced jet noise from becoming dominant, suppressor nozzles should, if possible, be designed to ventilate or somehow decay the velocity of the central jets in the cluster as rapidly as in the outer jets where mixing with surrounding air occurs. This would maximize the jet shielding effect.

Figures 9(a), 9(b), and 13 lead one to conclude that the jet shielding mechanism is related to disruption or absorption of sound waves by the convective kinetic energy of the molecules in the mixing zones. Shielding action appears to begin with jet velocities considerably below sonic and except for the ambient temperature case, it maximizes at approximately a jet Mach number of 1.1. With coalesced jet noise excluded, the shielding action continues to improve at higher jet Mach numbers. This effect is thought to be more due to the geometric expansion of the mixing zones (decreasing θ) rather than to increased disruption of sound waves in the mixing zones.

Of the other possible mechanisms to explain multitube noise suppression, shock interactions can be ruled out because of the large suppressions achieved sub-sonically at the higher jet temperatures (Fig. 9(b)). Other possibilities, such as jet interactions, cancellations, reduced noise generation because of reduced shear in the center of the cluster, etc., cannot really be differentiated from the concept of shielding, on the basis of the available data.

CONCLUDING REMARKS

The present assessment of jets as acoustic shields, using recent systematic data for single and multitube suppressor nozzles, and applying a simple geometric shielding hypothesis, has presented a strong case for jet shielding as being the sound-suppression mechanism operating in multitube nozzles whenever the jet velocities are near-sonic or above. The underlying hypothesis is that noise from a central jet in the cluster is effectively disrupted or absorbed in the high velocity mixing region around the jets in the outer row. At jet velocities above about 2000 ft/sec, the reduced suppression or shielding effect has been analyzed as being actually better shielding in the initial mixing region but with a progressive shift in the dominant noise source to the downstream large coalesced jet region.

The general equation derived from geometric shielding concepts for calculating the equivalent number of single tubes for a multitube suppressor nozzle is in excellent agreement with the data for the initial mixing region, and appears to predict a noise floor that represents complete shielding. Based on total sound power, and including the coalesced jet noise, the minimum number of equivalent tubes for the 37-tube nozzles tested is approximately 7 tubes.

Similar studies on nozzles different from the present 37-tube configuration are needed to explore the shielding model further and to aid in designing improved suppressor nozzles to better utilize shielding effects.

NOMENCLATURE

A_e	effective nozzle exhaust area
a_o	ambient speed of sound
D	diameter of nozzle or tube
F_j	shock noise parameter defined in reference 13
f	frequency
g	gap between adjacent tubes
M_j	jet Mach number, ideal
N	equivalent number of single tubes
N_P	number of tubes in outer row of tube bundle
PR	pressure ratio across nozzle
PWL	sound power level
PWL_f	sound power level in particular 1/3 octave band
PWL_T	total sound power level
PWL_{37}	total sound power level for 37-tube nozzle
PWL_1	total sound power level for single-tube nozzle
S	jet spreading slope, lateral to axial slope of outside edge of mixing zone (Fig. 2)
V_{av}	jet velocity, average at exit
V_{id}	jet velocity, ideal (γ = f (temp., fuel/air ratio), discharge coefficient = 1.0)
x	downstream distance from jet exit
θ	angle defined in Figure 2
ρ_o	ambient density

REFERENCES

1. Richards, E. J., "Jet Engine Noise," Journal of the Royal Aeronautical Society, Vol. 58, No. 520, pp. 221-223, 1954.

2. Greatrex, F. B., "Jet Noise," Fifth International Aeronautical Conference, IAE & RAS, 1955, pp. 415-448.

3. Callaghan, E. E., Howes, W., and North, W., "Tooth-Type Noise-Suppression Devices on a Full-Scale Axial-Flow Turbojet Engine," RM E54B01, 1954, NACA.

4. Ciepluch, C. C., North, W. J., Coles, W. D., and Antl, R. J., "Acoustic, Thrust, and Drag Characteristics of Several Full-Scale Noise Suppressors for Turbojet Engines," TN 4261, 1958, NACA.

5. Greatrex, F. B., "Noise Suppressors for Avon and Conway Engines," Engineering Societies Library, 59AV49, 1959.

6. Coles, W. D., "Jet Engine Exhaust Noise from Slot Nozzles," TN D-60, 1959, NASA.

7. Rollin, V. G., "Effect of Multiple-Nozzle Geometry on Jet-Noise Generation," TN D-770, 1961, NASA.

8. Eldred, K. E., White, R., Mann, M., and Cottis, M., "Suppression of Jet Noise with Emphasis on the Near Field," WPAFB ASD-TDR-62-578, 1963.

9. Nagamatsu, H. T., Sheer, R. E., Jr., and Bigelow, E. C., "Subsonic and Supersonic Jet Flow and Characteristics and Supersonic Suppressors," G.E. Rept. No. 72CRD264, Sept. 1972.

10. Atvars, J., Paynter, G. C., Walker, D. Q., and Wintermeyer, C. F., "Development of Acoustically Lined Ejector Technology for Multitube Jet Noise Suppressor Nozzles by Model and Engine Tests Over a Wide Range of Jet Pressure Ratios and Temperatures," Boeing Report, D6-60226, Contr. NAS3-15570, 1973.

11. Middleton, D., and Clark, P. J. F., "Assessment and Development of Methods of Acoustic Performance Prediction for Jet Noise Suppressors," U. of Toronto, UTIAS TN 134, AFOSR 69-0780 TR, 1969.

12. Wright, C. P., Morden, D. B., and Simcox, D. E., "SST Technology Follow-On Program - Phase I, A Summary of the SST Jet Noise Suppression Test Program," Boeing Final Report D6-60241, Contr. DOT-FA-SS-71-12, 1972.

13. von Glahn, Uwe H., "Correlation of Total Sound Power and Peak Sideline OASPL from Jet Exhausts," TM X-68059, 1972, NASA.

14. Nagamatsu, H. T., and Sheer, R. E., Jr., "Flow, Thrust, and Acoustic Characteristics of 50 Tubes with 50 Shrouds Supersonic Jet Noise Suppressor," Gen. Elect. Rept. No. 71C-258, 1971.

15. Nagamatsu, H. T., and Harvay, G., "Supersonic Jet Noise," Gen. Elect. Rept. No. 69C-161, 1969.

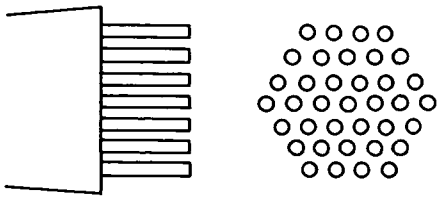

Figure 1. - 37 Tube suppressor nozzle array.

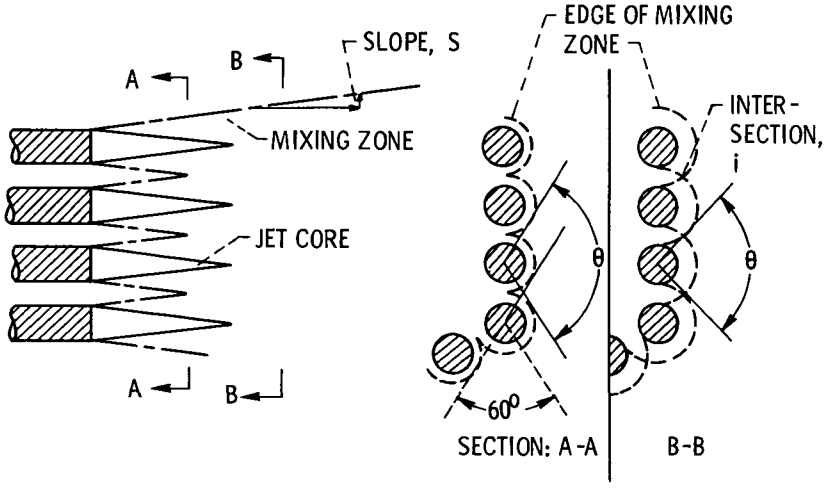

Figure 2. - Outer row of jets.

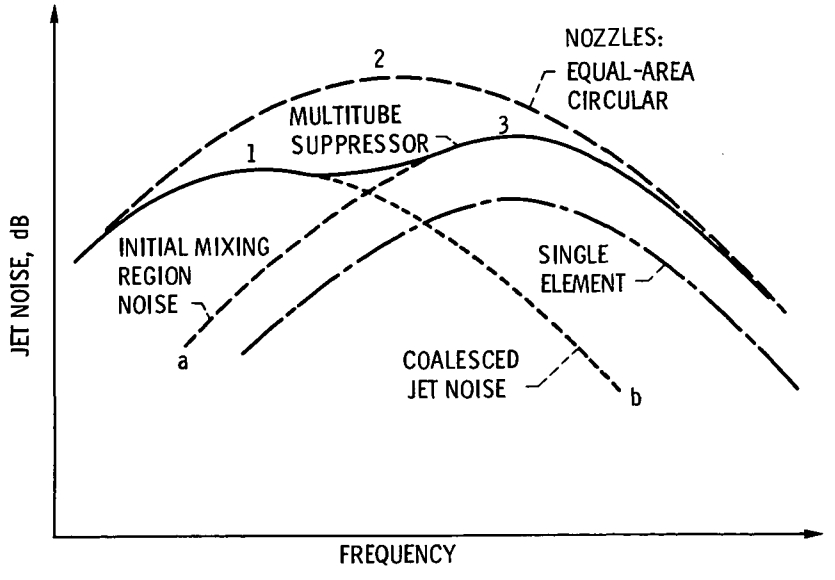

Figure 3. - Jet noise spectra.

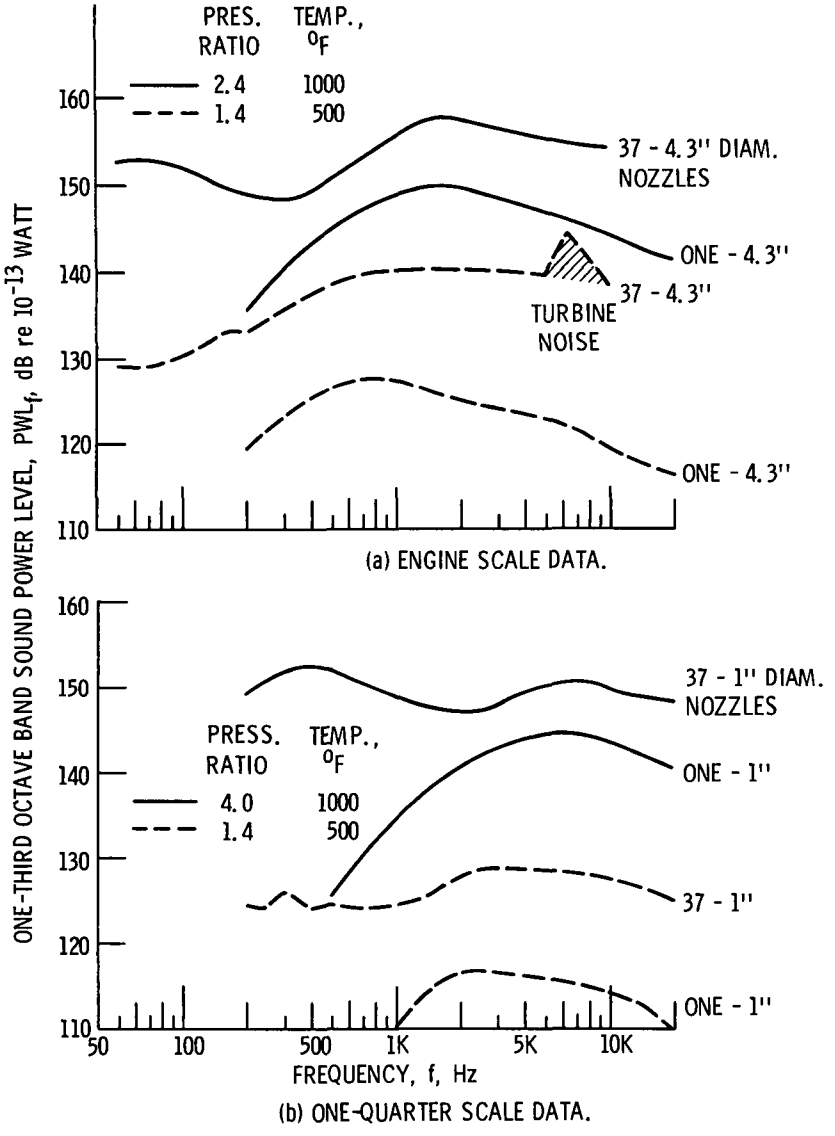

Figure 4. - Sound power spectra for single and multitube nozzles.

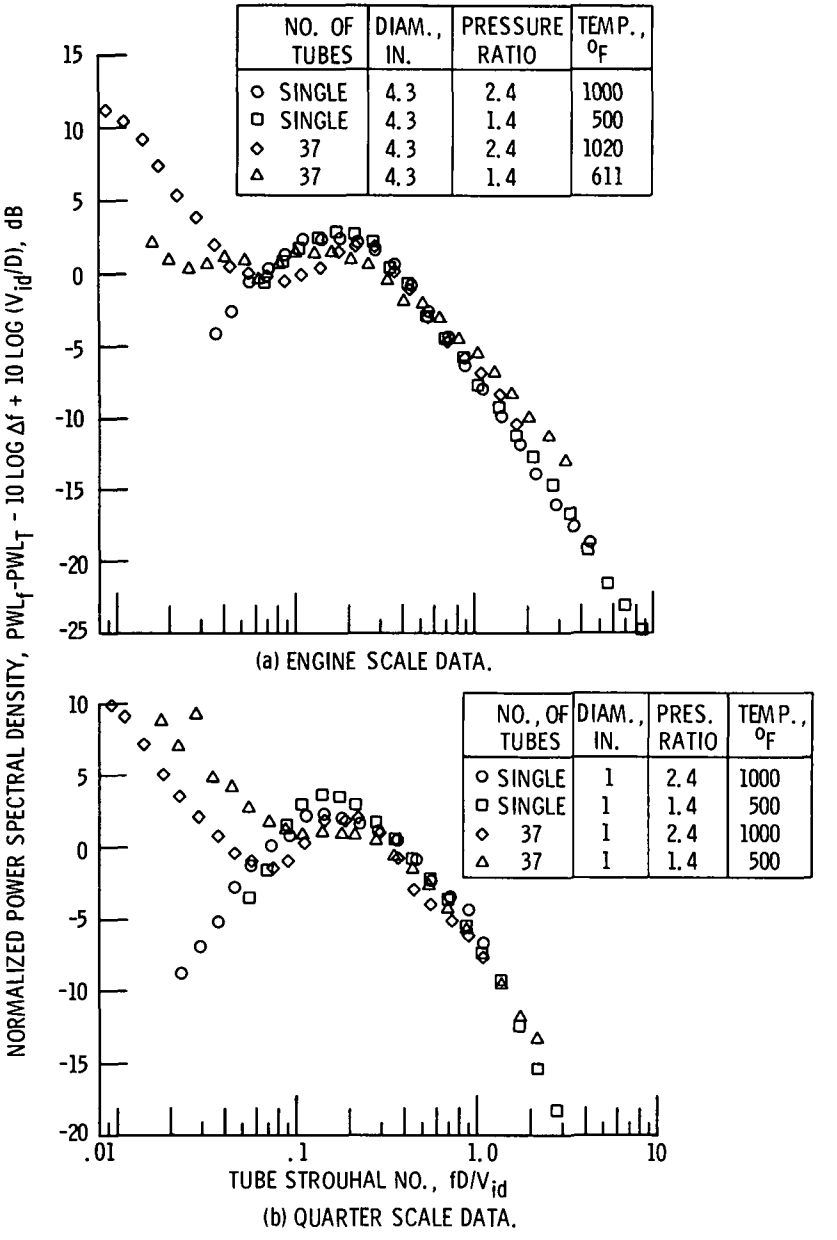

Figure 5. - Strouhal number distribution for single and multitube nozzles.

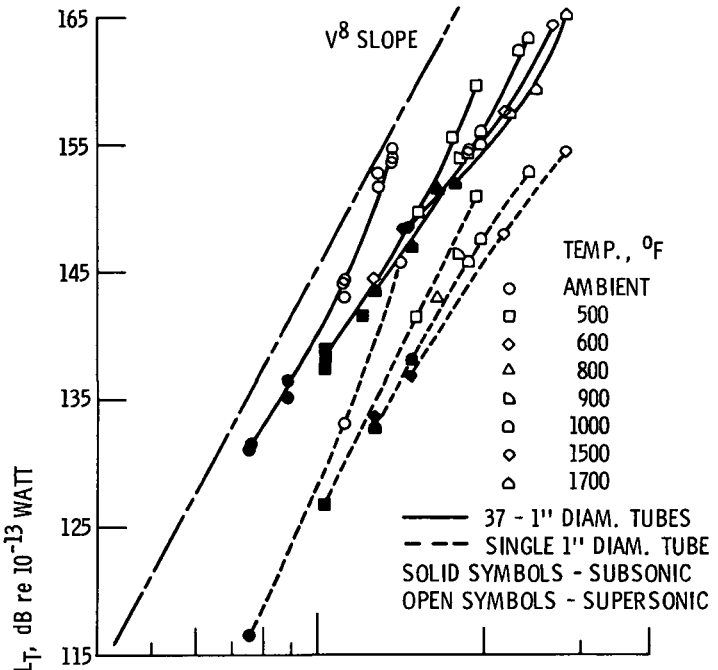

(a) QUARTER SCALE NOZZLES.

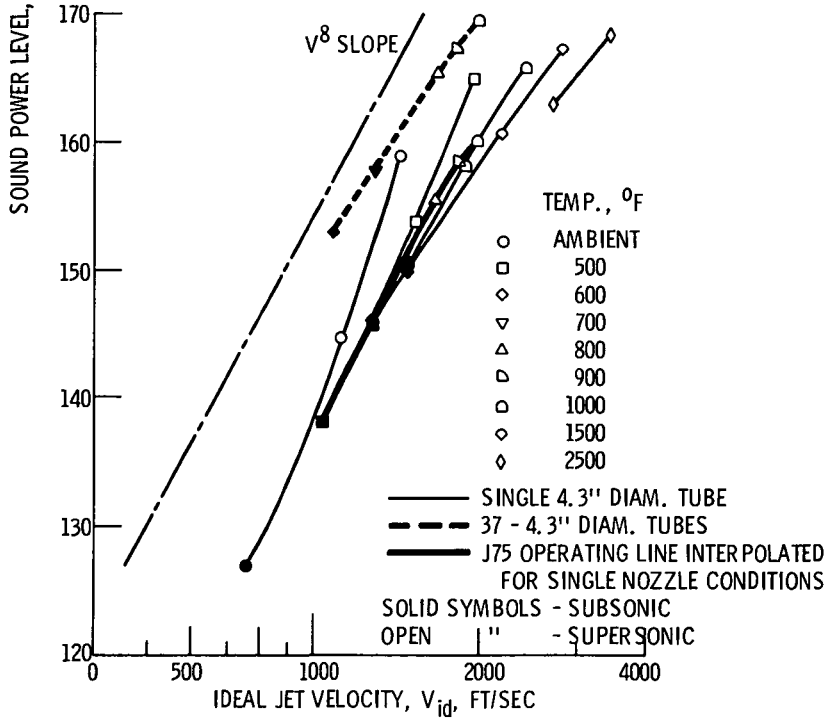

(b) ENGINE SCALE NOZZLES.

Figure 6. - Sound power level variation with jet velocity and temperature.

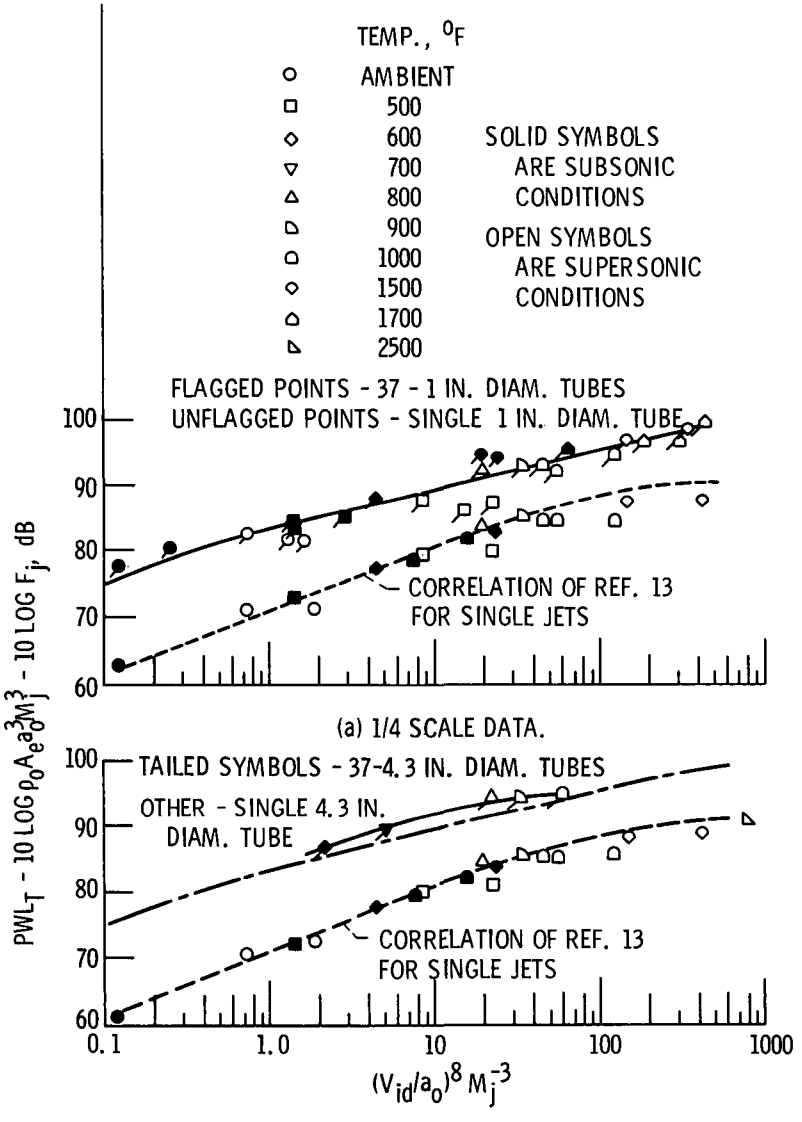

(a) 1/4 SCALE DATA.

(b) ENGINE SCALE DATA.

Figure 7. - Correlation of sound power levels for single and 37-tube nozzles.

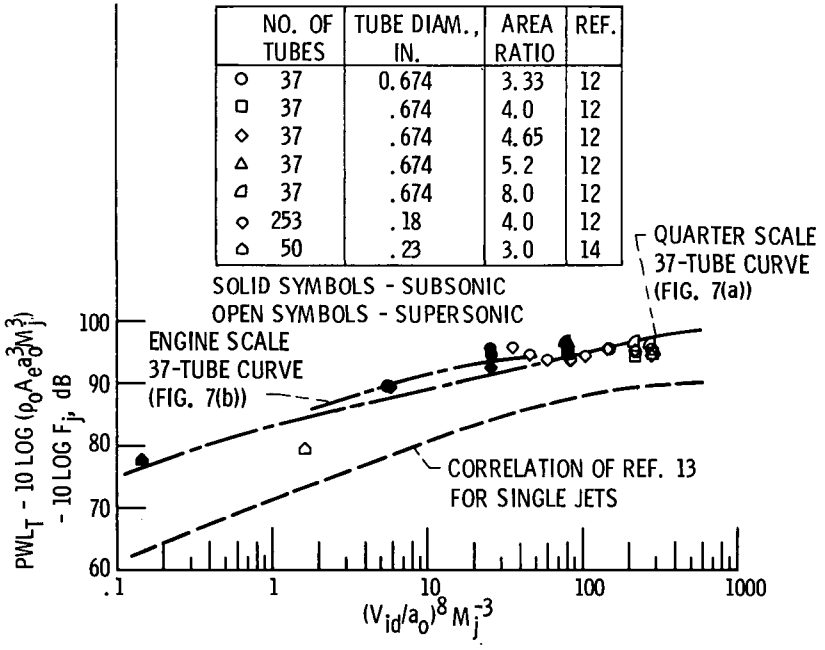

Figure 8. - Comparison of sound power levels for other multitube nozzles.

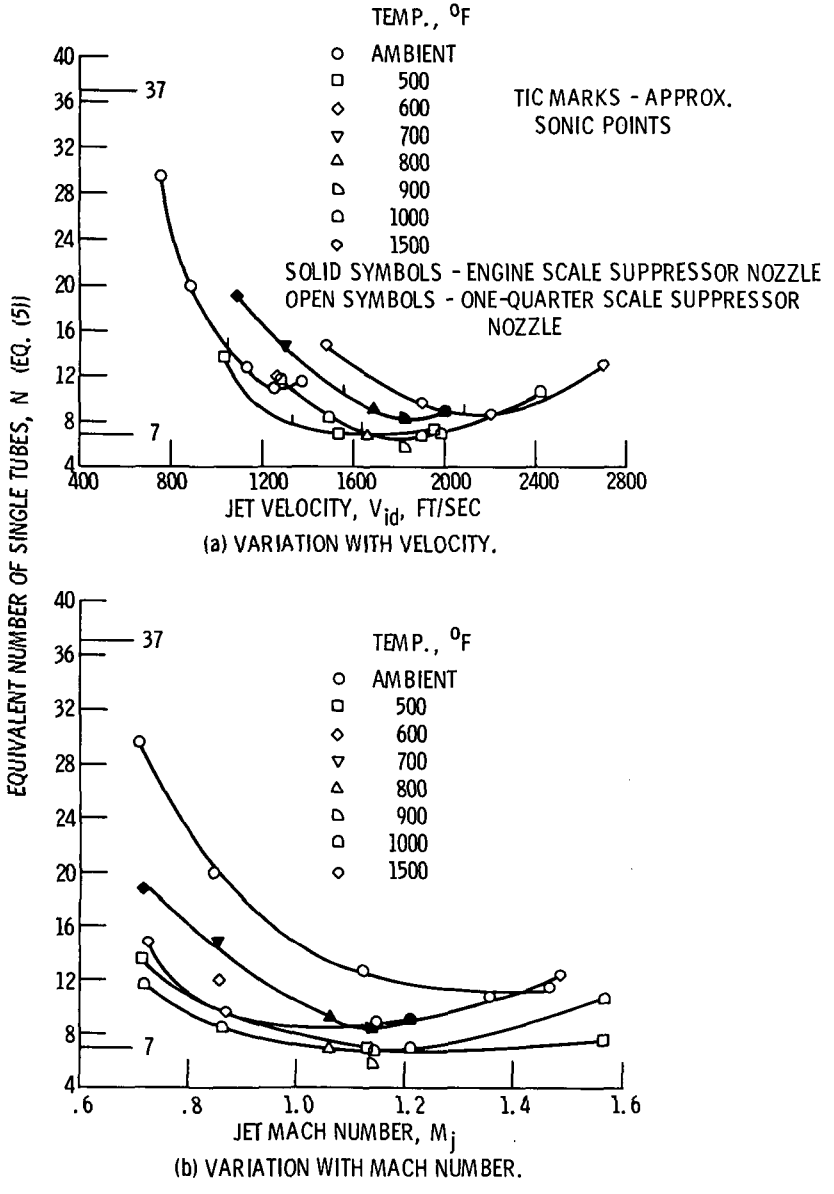

Figure 9. - Sound power of 37-tube suppressor nozzles expressed as equivalent number of single tubes.

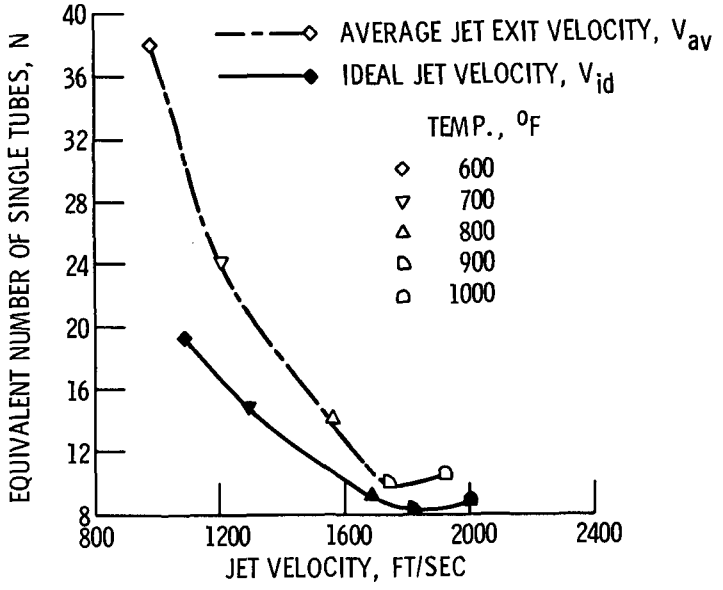

Figure 10. - Effect on equivalent tube number N of jet velocity definition. Engine scale data.

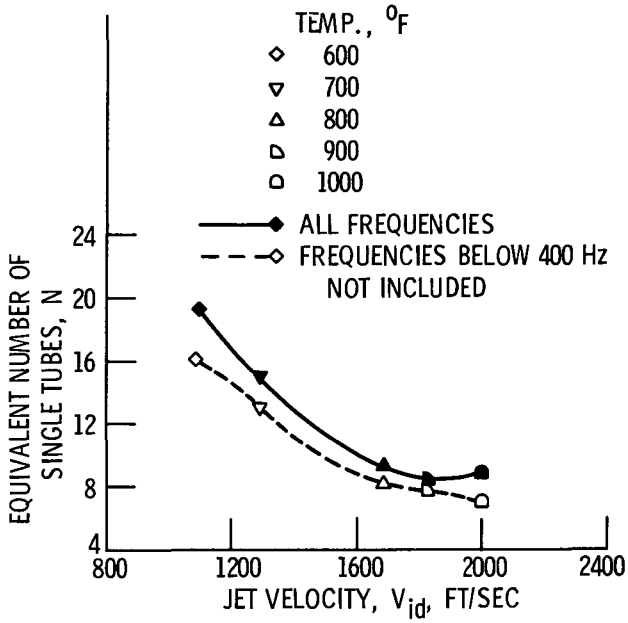

Figure 11. - Effect of exclusion of coalesced jet noise from equivalent tube number calculation. Engine scale data based on ideal jet velocity.

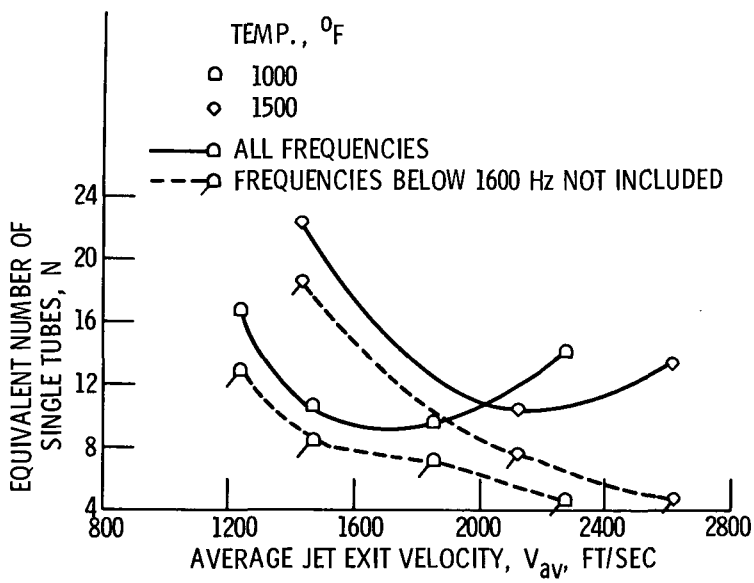

Figure 12. - Effect at high velocities of exclusion of coalesced jet noise from equivalent tube number calculation. Quarter scale data based on average jet velocity.

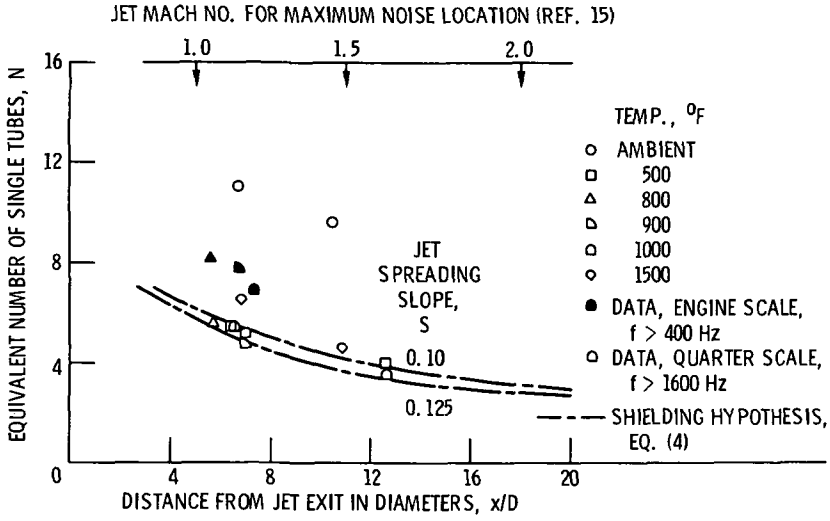

Figure 13. - Comparison of geometric hypothesis of jet shielding with supersonic jet acoustic data exclusive of coalesced jet noise.